

Electronic Absorption Spectra of C₃Cl, C₄Cl, and Their Ions in Neon MatricesJennifer van Wijngaarden,[†] Ivan Shnitko, Anton Batalov, Przemyslaw Kolek, Jan Fulara,[‡] and John P. Maier*

Department of Chemistry, University of Basel, Klingelbergstrasse 80, CH-4056 Basel, Switzerland

Received: March 23, 2005; In Final Form: April 25, 2005

Electronic absorption spectra of C₃Cl, C₃Cl⁺, C₃Cl[−], C₄Cl, and C₄Cl⁺ have been recorded in 6 K neon matrices following mass selection. Ab initio calculations were performed (CCSD(T) and CASSCF) to identify the ground and accessible excited states of each molecule. The estimated excitation energies and transition moments aid the assignment. The absorptions observed for C₃Cl are the $5^2A' \leftarrow X^2A'$ and $3^2A'' \leftarrow X^2A'$ transitions of the bent isomer and the $^2A_1 \leftarrow X^2B_2$ transition of the cyclic form in the UV (336.1 nm), visible (428.7 nm), and near-IR (1047 nm) regions, respectively. The band systems for bent C₃Cl[−] (435.2 nm) and linear C₃Cl⁺ (413.2 nm) are both in the visible region and correspond to $2^1A'' \leftarrow X^1A'$ and $^1\Pi \leftarrow X^1\Sigma^+$ type transitions. The C₄Cl and C₄Cl⁺ chains are linear, and the band origins of the $2^2\Pi \leftarrow X^2\Pi$ and $2^3\Pi \leftarrow X^3\Pi$ electronic transitions are at 427.0 and 405.7 nm. The spectral assignments are supported by analysis of the vibrational structure associated with each electronic transition.

Introduction

A number of carbon chains terminated by the second row elements—Si, P, and S—have been experimentally and theoretically investigated in recent years due to the detection of the shorter chains in astrophysical environments.¹ The chlorine containing analogues are likewise gaining interest and are thought to be good candidates for astronomical detection, as it is predicted that C—Cl bonds can be formed under interstellar conditions.² Furthermore, spectroscopic studies of heteroatom-terminated carbon chain molecules serve as tests of current theoretical models through the identification of periodic trends in molecular properties as a function of the end atom and chain length.

The ground state electronic structures and vibrational frequencies have been determined for the C_{*n*}Cl, C_{*n*}Cl[−], and C_{*n*}Cl⁺ (*n* = 1–7) molecules using DFT (B3LYP).^{3,4} For all but C₃Cl, the lowest energy structures are thought to be linear or quasilinear chains terminated on one end by the chlorine atom. In the case of C₃Cl, geometry optimization calculations suggest that the ground state structure is a cyclic triatomic carbon ring with an exocyclic chlorine (2B_2) C_{2_v}; however, quasilinear ($^2A'$) C_s and linear ($^2\Pi$) structures are estimated to lie only 12 kJ/mol higher in energy.⁵ For the larger species, the calculated C—C bond distances suggest that the most important valence structures are cumulenic, although the observation of bond length alternation suggests that polyynic ones also contribute, particularly for the *n* = even chains. The ab initio results further predict that the C_{*n*}Cl and C_{*n*}Cl⁺ chains exhibit alternating stability depending on whether *n* is even or odd. For the neutral species, the *n* = even chains are predicted to be more stable than the *n* = odd ones, but the trend is reversed for the corresponding cations.

Experimentally, the CCl radical is the most extensively studied of the C_{*n*}Cl species and spectra have been reported in the microwave,⁶ infrared,^{7–9} and ultraviolet regions.^{10–12} High resolution gas phase spectroscopic studies have been conducted for other small molecules of this type such as the CCl⁺ cation¹³ and the C₂Cl radical,¹⁴ and recently, the absorption spectra of the longer chains—C₅Cl, C₅Cl⁺, C₆Cl, and C₆Cl⁺—were reported in neon matrices.¹⁵ Spectroscopic investigations of the intermediate chlorine-terminated carbon chain molecules will bridge the gap in the existing experimental data and will further provide a test of the current theoretical results for this series of molecules.³

In this paper, the first spectroscopic study of C₃Cl and C₄Cl and their ions, C₃Cl[−], C₃Cl⁺, and C₄Cl⁺, using mass-selective neon matrix isolation spectroscopy is reported. The band assignments of each molecule are based upon ab initio predictions of the expected electronic transitions and ground state vibrational frequencies. The spectral assignments are further supported by comparisons with the previously reported spectra of the longer C_{*n*}Cl and C_{*n*}Cl⁺ (*n* = 5, 6) chains and with the isoelectronic species C_{*n*}S and C_{*n*}S[−], as appropriate.¹⁶

Experimental Method

The electronic absorption spectra of the C_{*n*}Cl (*n* = 3, 4) species and their ions were recorded following mass-selective deposition in neon matrices using the described instrument.¹⁷ A gas mixture containing the appropriate precursor was prepared by passing helium over a liquid sample of *c*-C₃Cl₄ or C₄Cl₆. From these respective mixtures, a number of C₃Cl_{*m*}⁺ and C₄Cl_{*m*}⁺ cations were produced, along with the corresponding neutral and anionic species, using a hot cathode discharge source. The cation beam was focused and directed into a quadrupole mass filter using a series of electrostatic optics.¹⁸ The C₃Cl⁺ or C₄Cl⁺ cations were selected with a mass resolution of ± 2 amu for each experiment, and the typical ion currents achieved were 44 and 75 nA for the two species, respectively.

The mass-selected cations were deposited simultaneously with neon on a rhodium-coated sapphire substrate over a period of

* Corresponding author. E-mail: J.P.Maier@unibas.ch. Phone: +41 61 267 38 26. Fax: +41 61 267 38 55.

[†] Current address: Department of Chemistry, Mount Holyoke College, 50 College St., South Hadley, MA, 01075.

[‡] Permanent address: Instytut Fizyki Polskiej Akademii Nauk, Al. Lotników 32-46, 02-668 Warsaw, Poland.

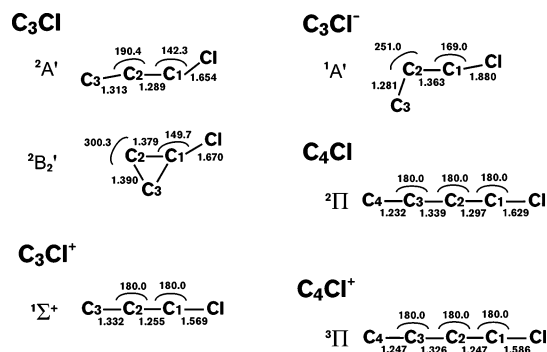


Figure 1. Calculated structural parameters for the observed electronic states of the C_nCl species at the CCSD(T)/cc-pVTZ level. Bond lengths are given in angstroms and bond angles in degrees.

3 h to produce a 6 K matrix. Due to a high incidence of electron recombination and molecular dissociation events in the matrix, additional measures were necessary to suppress these processes so that the desired species could be spectroscopically probed. During the deposition of C_3Cl^+ ions, a positive potential of 25 V was applied to the matrix to slow the approaching ions and reduce fragmentation. To suppress the neutralization of C_3Cl^+ and C_4Cl^+ , small concentrations of N_2O or CCl_4 were added to the neon gas in ratios of approximately 1:250. These impurities served as scavengers by removing free electrons that were attracted to the positively charged matrix after liberation from surrounding metal surfaces.

The samples were irradiated with monochromatic light from halogen and xenon arc lamps with beams running parallel to the substrate surface. Absorption spectra of the trapped species were recorded between 220 and 1100 nm using photomultiplier and silicon diode detectors. Spectra in the 12 000–1100 cm^{-1} range were recorded after sampling the neon matrix by a Fourier transform spectrometer, whereby the light was passed twice through the ~ 150 μm thickness of the matrix being reflected off the rhodium substrate. The matrix samples were then exposed to filtered radiation ($\lambda > 305$ nm) from a medium pressure mercury lamp and later to the full radiation (including $\lambda < 305$ nm) of this lamp as a next step. After each irradiation step, a spectrum was recorded to distinguish transitions of stable species from those of ions and photounstable molecules.

Computational Method

An ab initio study of C_3Cl , C_3Cl^+ , C_3Cl^- , C_4Cl , and C_4Cl^+ was performed using the MOLPRO software package¹⁹ with cc-pVTZ basis sets described in more detail elsewhere.²⁰ To start, the ground state geometries were optimized using the CASSCF and CCSD(T) methods for comparison. Once the geometries were determined, vertical excitation energies and transition moments were computed for several excited states simultaneously using CASSCF with state-averaged orbitals. Both quasilinear and cyclic structures were considered, as previous theoretical work predicted that their ground state energies were similar for C_3Cl .⁵

Results and Discussion

(a) C_3Cl . After mass selection, C_3Cl^+ was co-deposited with an excess of neon to form a 6 K matrix and the absorption spectrum was recorded. This reveals three clear systems in the UV, visible, and near-IR regions with band origins at 336.1, 428.7, and 1047 nm, respectively. These are attributed to the C_3Cl molecules formed by neutralization of the cationic precursor in the matrix. The assignment is supported by the

TABLE 1: Electronic Excitation Energies of C_3Cl and C_4Cl and Their Ions Computed with CASSCF/cc PVTZ

	excited state	excitation energy		transition moment/D		
		experimetal (adiabatic)	CASSCF (vertical)			
				a	b	c
<i>b</i> -C ₃ Cl						
X ² A'	1 ² A'		2.60	0.051	0.631	
	2 ² A'		3.34	0.158	0.198	
	3 ² A'		4.02	−0.002	0.248	
	4 ² A'		4.30	−0.409	0.099	
	5 ² A'	3.70	4.55	0.961	0.121	
	6 ² A'		5.73	0.529	0.050	
	1 ² A''		0.64		−0.230	
	2 ² A''		2.69		−0.219	
	3 ² A''	2.89	3.06		−0.809	
	4 ² A''		3.79		0.003	
	5 ² A''		4.03		0.180	
	6 ² A''		5.04		0.086	
	7 ² A''		5.42		−0.185	
	8 ² A''		5.67		−0.156	
<i>c</i> -C ₃ Cl						
X ² B ₂	1 ² A ₁	1.18	1.48	−1.789		
	1 ² B ₁		3.64	forbidden		
	1 ² A ₂		4.00		0.362	
	2 ² B ₁		4.29	forbidden		
	2 ² A ₂		5.29		−0.857	
	2 ² A ₁		5.59	0.85		
	1 ² B ₂		5.76	−1.22		
<i>b</i> -C ₃ Cl [−]						
X ¹ A'	1 ¹ A'		4.11	−0.276	0.533	
	2 ¹ A'		4.35	0.075	−0.455	
	3 ¹ A'		4.72	0.007	0.147	
	1 ¹ A''		2.03			−0.589
	2 ¹ A''	2.85	3.23			1.203
	3 ¹ A''		3.96			−0.078
<i>l</i> -C ₃ Cl ⁺						
X ¹ Σ ⁺	1 ¹ Π	3.00	3.29	−0.775	−0.775	
	1 ¹ Δ		3.78	forbidden		
<i>l</i> -C ₄ Cl						
² Π	2 ² Π	2.90	3.34	1.670		
	2 ² Σ ⁺		5.27		0.660	0.660
<i>l</i> -C ₄ Cl ⁺						
³ Π	1 ³ Δ		2.54		0.136	0.136
	2 ³ Σ ⁺		2.60		0.129	0.129
	2 ³ Π	(2.87), 3.06	2.92	2.553		

observation that the bands increased in intensity after UV irradiation, as positively charged molecules are known to be neutralized under these conditions.

The lowest energy C_3Cl isomer is cyclic C_{2v} in the X^2B_2 electronic state, although a bent isomer lies only 17.4 kJ/mol higher in energy at the CCSD(T) level (present work) and 12 kJ/mol higher according to DFT calculations.⁵ The nonlinear structure is similar to that reported earlier (DFT/B3LYP and QCISD) but with a greater deviation from linearity in the C–C–Cl angle ($142.3^\circ/144.0^\circ$ from CCSD(T) and CASSCF). Because the species in the matrix are produced via neutralization of the linear C_3Cl^+ precursor, it was expected that the chain isomer of C_3Cl would be the primary neutral constituent of the sample even though the cyclic form is lower in energy. The excitation energies and transition moments of the allowed electronic transitions less than 6 eV are listed in Table 1 for both isomers, and the calculated ground state structures are shown in Figure 1.

A rich vibrational structure is observed for the UV band of C_3Cl in Figure 2 and is attributed to the $5^2A' \leftarrow X^2A'$ transition of the bent isomer; the vibrational assignments are listed in Table 2. This is predicted to have a large transition moment, and the observed band origin at 336.1 nm falls 0.86 eV below the ab initio prediction. The discrepancy is partially explained by the fact that the comparison is between vertical and adiabatic

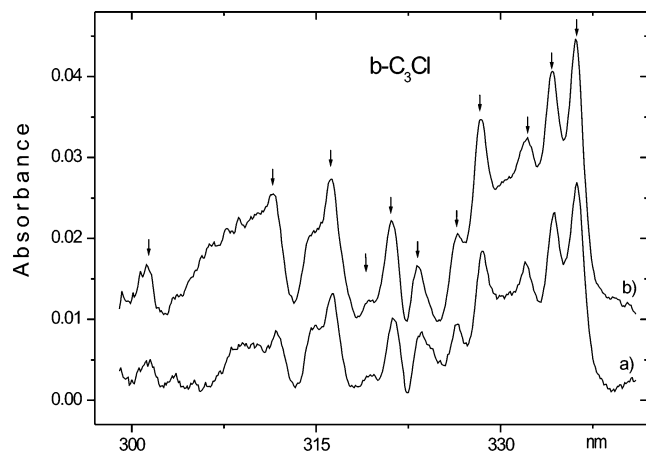


Figure 2. Electronic absorption spectra of the $5^2A' \leftarrow X^2A'$ transition of bent C₃Cl in the UV region. The spectra were recorded in a 6 K neon matrix both (a) before and (b) after UV irradiation ($\lambda > 305$ nm).

TABLE 2: Positions of the Band Maxima (± 0.2 nm) Observed for Electronic Transitions of C₃Cl, C₃Cl[−], and C₃Cl⁺ in 6 K Neon Matrixes

species	λ/nm	ν/cm^{-1}	$\Delta\nu/\text{cm}^{-1}$	assignment
<i>b</i> -C ₃ Cl				
$5^2A' \leftarrow X^2A'$	336.1	29 753	0	0_0^0
	334.2	29 922	169	ν_6
	332.2	30 102	349	$2\nu_6$
	328.4	30 451	698	ν_3
	326.5	30 628	875	$\nu_3 + \nu_6$
	323.3	30 931	1178	ν_2
	321.1	31 143	1390	$2\nu_3$
	319.2	31 328	1575	$2\nu_3 + \nu_6$
	316.2	31 626	1873	ν_1
	314.7	31 776	2023	$\nu_1 + \nu_6$
	311.5	32 103	2350	$2\nu_2$
	301.3	33 190	3437	$3\nu_2$
$3^2A'' \leftarrow X^2A'$	428.7	23 326	0	0_0^0
	423.9	23 590	264	ν_5
<i>c</i> -C ₃ Cl				
$1^2A_1 \leftarrow X^2B_2$	1047	9552	0	0_0^0
	987.5	10 127	576	ν_4
	958.5	10 433	882	$2\nu_6$
	951.5	10 510	959	$2\nu_5$
	937.2	10 670	1119	ν_2
	910.2	10 987	1436	$2\nu_3$
	896.2	11 158	1607	ν_1
	883.5	11 319	1768	$4\nu_6$
	878.2	11 387	1836	$4\nu_5$
	865.7	11 551	2000	$2\nu_3 + \nu_4$
<i>b</i> -C ₃ Cl [−]				
$2^1A'' \leftarrow X^1A'$	435.2	22 978	0	0_0^0
	418.0	23 923	945	ν_2
<i>l</i> -C ₃ Cl ⁺				
$1^1\Pi \leftarrow X^1\Sigma$	413.2	24 201	0	0_0^0
IR:	<i>l</i> -C ₃ Cl ⁺	$\nu_1 = 2142.6 \text{ cm}^{-1}$,	<i>b</i> -C ₃ Cl	$\nu_1 = 1859.1 \text{ cm}^{-1}$

excitation energies which typically differ by ~ 0.2 – 0.3 eV. The remaining error may be attributed to the limitations of the CASSCF method which often produces unusually large correlation energies for higher excited states.

The observed vibrational bands in Figure 2 correspond to the excitation of four vibrational modes of C₃Cl as well as to their combinations and overtones. At 6 K, the molecules are primarily in the lowest vibrational level of the ground state, and thus, the observed progression is due to excitation of carbon chain stretching and bending modes ($\nu_1 = 1873$, $\nu_2 = 1178$, $\nu_3 = 698$, $\nu_6 = 169 \text{ cm}^{-1}$) in the excited electronic state of C₃Cl. The values compare favorably with the frequencies computed via ab initio methods for the ground electronic state (B3LYP/6-311G+(d): $\nu_1 = 1932$, $\nu_2 = 1338$, $\nu_3 = 672$, $\nu_6 = 176 \text{ cm}^{-1}$).³ The IR spectrum of C₃Cl was also measured in its ground

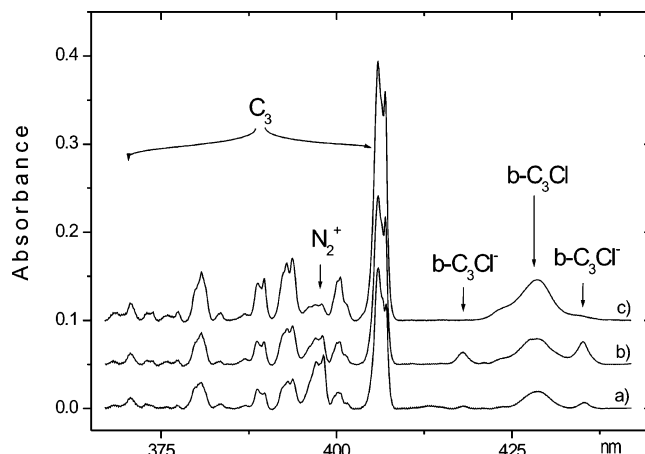


Figure 3. Electronic absorption spectra in the visible region of the $3^2A'' \leftarrow X^2A'$ transition of bent C₃Cl and the $2^1A'' \leftarrow X^1A'$ transition of bent C₃Cl[−] in 6 K neon matrixes. The traces show the observed spectra (a) after deposition, (b) after exposure to UV wavelengths ($\lambda > 305$ nm), and (c) after irradiation with a broader spectrum (including $\lambda < 305$ nm). Both C₃ and N₂⁺ present in the matrix absorb in this spectral region.

electronic state revealing only the ν_1 band (1859.1 cm^{-1}) which differs by 14 cm^{-1} from the excited state vibrational frequency extracted from the electronic spectrum (Figure 2).

A second band of the bent C₃Cl radical is observed in the visible region at 428.7 nm (Figure 3) and is assigned to the origin of the $3^2A'' \leftarrow X^2A'$ system in Table 2. This is predicted to be the second strongest transition of this isomer and lies within 0.17 eV of the theoretical prediction. A smaller band, blue-shifted by 264 cm^{-1} , is assigned to the ν_5 vibrational mode in the excited electronic state based on the ab initio estimate of ground state fundamental frequency ($\nu_5 = 227 \text{ cm}^{-1}$). Additional vibrational bands may be present, but their assignment is precluded by the strong C₃ and N₂⁺ absorptions in this spectral region. The excitation of one quantum of ν_1 stretch, for example, would result in a band at 397 nm in Figure 3 which overlaps with the N₂⁺ absorption.

The third electronic transition of the C₃Cl radical is considerably weaker than the others and appears in the near-IR (NIR) region. This absorption is attributed to a cyclic C_{2v} isomer where the chlorine atom is bonded to a triatomic carbon ring. The band origin at 1047 nm in Figure 4 is assigned to the $2^2A_1 \leftarrow X^2B_2$ transition of *c*-C₃Cl and is 0.28 eV lower in energy than the theoretical estimate. The observed vibrational pattern supports the assignment of this band to the cyclic isomer, as the progression involves all six vibrational modes of *c*-C₃Cl (Table 2). The experimentally observed frequencies for the 2^2A_1 state ($\nu_1 = 1607$, $\nu_2 = 1119$, $\nu_3 = 718$, $\nu_4 = 576$, $\nu_5 = 480$, $\nu_6 = 441 \text{ cm}^{-1}$) correlate well with the ab initio values determined in this work at the DFT B3LYP level for the 2^2B_2 ground state ($\nu_1 = 1650$, $\nu_2 = 1222$, $\nu_3 = 772$, $\nu_4 = 595$, $\nu_5 = 412$, $\nu_6 = 350 \text{ cm}^{-1}$). The largest discrepancies are for the low frequency modes which correspond to the C–C–Cl bending (ν_5 , ν_6) and C–Cl stretching modes (ν_4). The modes relating to ring deformation (ν_2 , ν_3) and stretching (ν_1) are in close agreement with the experimental values which lends strong support for the assignment of these bands to the cyclic isomer, *c*-C₃Cl.

An additional experiment was performed in which a matrix sample containing both structural isomers of C₃Cl was exposed to a broad spectrum of UV wavelengths and subsequently exposed to filtered light containing only longer wavelengths ($\lambda > 305 \text{ nm}$). The UV and visible bands of bent C₃Cl were

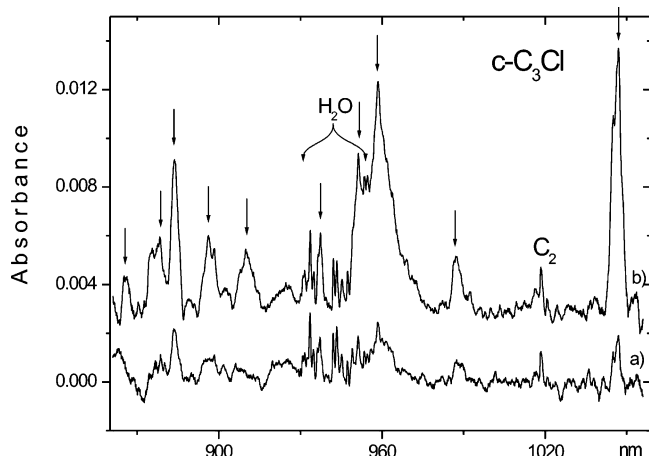


Figure 4. Near-IR band origin of the ${}^2A_1 \leftarrow X^2B_2$ electronic transition of $c\text{-C}_3\text{Cl}$ recorded in a 6 K matrix. The bands marked by arrows are assigned to this structural isomer. Trace a was recorded after the initial deposition of C_3Cl^+ and shows little $c\text{-C}_3\text{Cl}$. Trace b demonstrates that the spectrum becomes enriched in the cyclic isomer after stepwise UV irradiation ($\lambda > 305$ nm), as described in the text. The spectra also reveal the presence of H_2O vapor in the chamber and C_2 fragments.

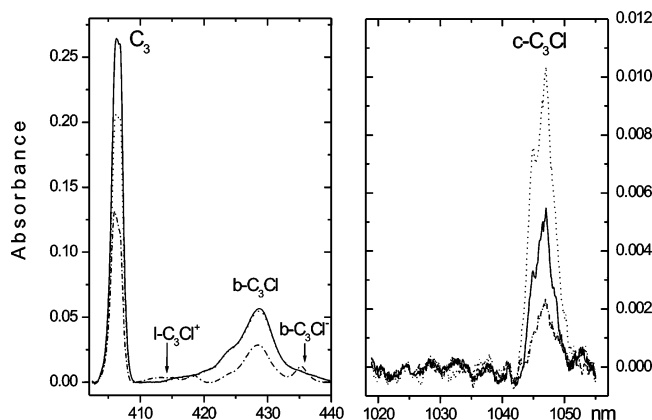


Figure 5. Comparison of the behavior of the origin bands of C_3 and $c\text{-C}_3\text{Cl}$ upon UV irradiation. The traces drawn with dashed–dotted lines show the bands immediately after the matrix is formed. After irradiation including high energy photons ($\lambda < 305$ nm), the bands assigned to C_3 and $c\text{-C}_3\text{Cl}$ increase in intensity (solid trace). Following a second irradiation involving only lower energy photons ($\lambda > 305$ nm), the C_3 band decreases and that due to $c\text{-C}_3\text{Cl}$ increases (dotted trace) in intensity, suggesting that the cyclic isomer of $c\text{-C}_3\text{Cl}$ is formed from C_3 .

only affected by the first irradiation, while the NIR band of $c\text{-C}_3\text{Cl}$ grew in intensity after both exposures, as seen in Figure 5. This increase in intensity of the cyclic isomer was accompanied by a simultaneous decrease in the intensity of the C_3 band at 407 nm. The $c\text{-C}_3\text{Cl}$ isomer therefore appears to be formed from C_3 , and the additional UV exposure must provide the energy for the transformation in the matrix.

(b) C_3Cl^- . During the assignment of the neutral C_3Cl species in Figure 3, two additional bands were observed at 435.2 and 418.0 nm which could not be attributed to neutral or cationic species. The transitions increased in intensity upon UV irradiation with longer wavelengths ($\lambda > 305$ nm) and then decreased when exposed to higher energy photons ($\lambda < 305$ nm). Absorption bands related to neutral molecules usually grow or remain constant in intensity as a result of each irradiation step, while those attributable to cations decrease. Exposure to UV light, however, can increase the number of sample anions by liberating electrons from weakly bound anions (e.g., OH^-) present in the matrix. When subsequently exposed to higher

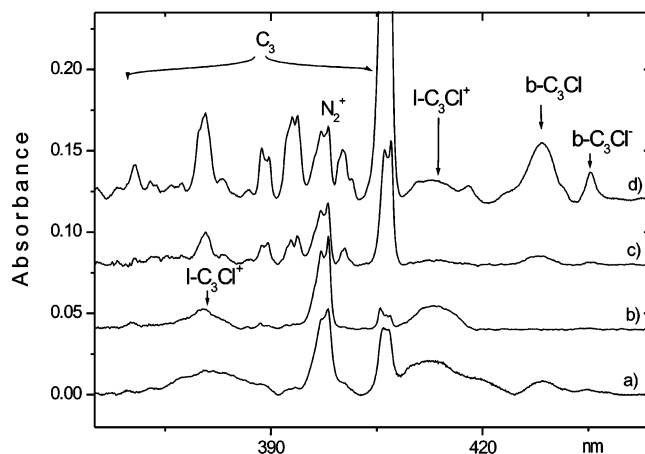


Figure 6. Band origin of the ${}^1\Pi \leftarrow X^1\Sigma^+$ electronic transition of C_3Cl^+ recorded in a 6 K matrix. Traces a and b show the spectrum recorded after deposition of C_3Cl^+ in a neon matrix containing 0.25% CCl_4 and N_2O , respectively. Trace c is the resulting spectrum after UV irradiation of the matrix sample containing the N_2O electron scavenger. Trace d was observed after deposition of low kinetic energy (~ 15 eV) cations (C_3Cl^+).

energy, the observed signal will decrease if the photons are of sufficient energy to detach electrons from the newly formed anions (e.g., C_3Cl^-) in the sample. This is precisely the behavior that was observed for the two additional bands in Figure 3. Evidence for the presence of anions in the matrix sample is the observation that the bands at 435.2 and 418.0 nm were suppressed when electron scavengers (CCl_4 or N_2O) were introduced into the matrix. These molecules have high electron affinities and restrict the formation of other molecular anions.

The lowest energy structure of C_3Cl^- is predicted to be bent (Figure 1), and the ground state electronic configuration corresponds to a singlet ${}^1A'$ state. The strongest electronic transition is estimated to be of the type $2^1A'' \leftarrow X^1A'$, with an energy of 3.23 eV (Table 1). This correlates well with the observed band at 435.2 nm (2.85 eV). The second band is blue-shifted by 945 cm^{-1} and is assigned to the excitation of the ν_2 vibrational mode in the $2^1A''$ state of C_3Cl^- in Table 2. The ground state vibrational frequency is predicted to be considerably higher (DFT, 1157 cm^{-1}), but the corresponding mode was similarly overestimated by ab initio calculations for the neutral C_3Cl counterpart (experiment, 1178 cm^{-1} ; DFT, 1338 cm^{-1}). The electron affinity of C_3Cl is estimated to be around 2.68 eV (CCSD(T)/aug-cc-pVTZ), but the anion appears to be stabilized in the matrix, as electron detachment is not observed until photons with energies greater than 4 eV are used.

(c) C_3Cl^+ . The first spectra recorded after mass-selected deposition of C_3Cl^+ ions with neon revealed no evidence of the cation in the matrix. This is a consequence of an efficient neutralization process whereby electrons liberated from nearby metal surfaces are attracted to the positively charged matrix. To observe the spectrum of C_3Cl^+ , it was necessary to mix the neon gas with a small amount of N_2O (250:1 ratio). Since N_2O is a good scavenger, the number of free electrons in the matrix was reduced and the concentration of C_3Cl^+ was sufficient for a spectroscopic study. Subsequently, a broad transition was observed at 413.2 nm (Figure 6) which disappeared upon UV exposure. The same band was observed when the kinetic energy of C_3Cl^+ being deposited was decreased through the application of a positive voltage to the matrix. The 413.2 nm band is consequently attributed to the C_3Cl^+ cation.

The ground state of linear C_3Cl^+ (Figure 1) is described by a singlet $X^1\Sigma^+$ electronic configuration, and the lowest energy

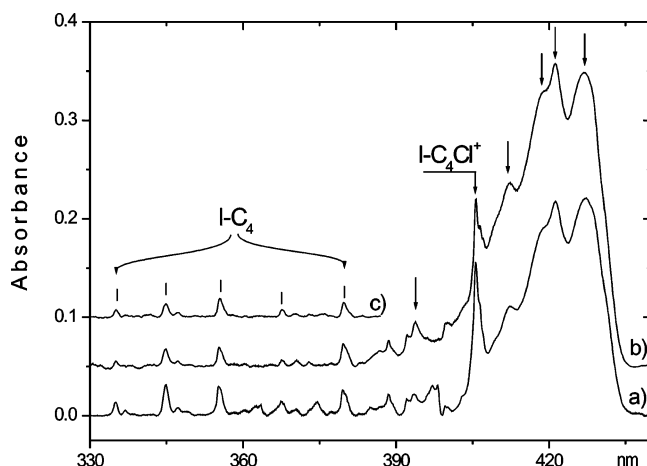


Figure 7. Electronic absorption spectra of the $2^2\Pi \leftarrow X^2\Pi$ electronic transition of C₄Cl recorded in a 6 K neon matrix both (a) before and (b) after UV irradiation. The transitions marked by arrows increased in intensity after exposure to UV light and are assigned to linear C₄Cl. Additional bands are due to C₄Cl⁺ and C₄. Trace c shows the linear C₄ absorptions after C₄⁺ mass-selected deposition and subsequent matrix neutralization.

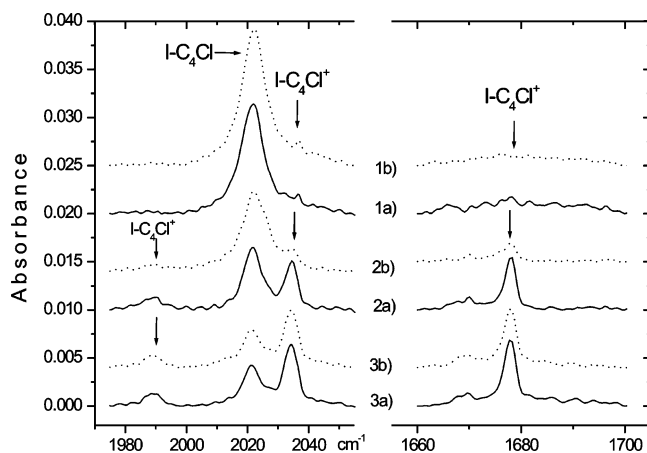


Figure 8. Infrared absorption spectra of C₄Cl and C₄Cl⁺ in neon matrices. The solid traces (1a, 2a, and 3a) are the spectra recorded in a pure neon matrix and in matrices containing 0.25% of the electron scavengers N₂O and CCl₄, respectively. The dotted traces (1b, 2b, and 3b) show the same bands after UV irradiation ($\lambda > 305$ nm).

transition involves electronic excitation to an antibonding orbital. For the analogous $\pi-\pi^*$ type excitations in linear C₅Cl and C₅Cl⁺, the band origins were observed in the UV region at 247.1 and 266.1 nm, respectively, in neon matrices.¹⁵ The $1^1\Pi \leftarrow X^1\Sigma^+$ transition of C₃Cl⁺ is predicted to be of lower energy, however, and the band at 413.2 nm is within 0.3 eV of the calculated transition (3.29 eV).

On the basis of DFT calculations of the ground electronic state of linear C₃Cl⁺, the most intense transition in the IR spectrum is predicted to be the ν_1 mode (2224 cm⁻¹),³ and this is consistent with the IR absorption spectrum of this matrix sample. A band is observed at 2142.6 cm⁻¹ which decreases in intensity when irradiated with wavelengths longer than 305 nm and disappears completely when exposed to shorter wavelengths, as expected for a cationic species. The electronic absorption spectrum of the related odd chain C₅Cl⁺ molecule was dominated by a vibronic progression arising from the excitation of the C–Cl stretch (486 cm⁻¹) in the excited electronic state.¹⁵ For C₃Cl⁺, this mode is predicted to have a higher frequency (690 cm⁻¹) and this vibronic band is expected to nearly coincide with a known transition of C₃.

TABLE 3: Positions of the Band Maxima (± 0.2 nm) Observed for Electronic Transitions of C₄Cl and C₄Cl⁺ in 6 K Neon Matrices

species	λ/nm	ν/cm^{-1}	$\Delta\nu/\text{cm}^{-1}$	assignment
<i>I</i> -C ₄ Cl $2^2\Pi \leftarrow X^2\Pi$	427.0	23 419		0_0^0
	421.3	23 736	317	ν_5
	418.8	23 878	459	ν_4
	412.3	24 254	835	$\nu_4 + \nu_5$
	393.8	25 394	1975	ν_1
<i>I</i> -C ₄ Cl ⁺ $2^3\Pi \leftarrow X^3\Pi$	405.7	24 649		0_0^0
	397.1	25 183	534	ν_4
	388.4	25 747	1098	$2\nu_4$
	378.1	26 448	1799	ν_2
	374.4	26 709	2060	ν_1
	366.8	27 263	2614	$\nu_1 + \nu_4$
	359.2	27 840	3191	$\nu_1 + 2\nu_4$
	355.0	28 169	3520	$2\nu_2$
	431.7	23 164		0_0^0
	420.6	23 776	612	ν_4

IR: *I*-C₄Cl $\nu_1 = 2022.1$ cm⁻¹; *I*-C₄Cl⁺ $\nu_1 = 2034.4$ cm⁻¹, $\nu_4 = 1678.0$ cm⁻¹

(d) C₄Cl. An analogous experiment was carried out by co-depositing mass-selected C₄Cl⁺ with neon to form a 6 K matrix, and the resulting electronic absorption spectrum is shown in Figure 7. The strong vibronic band system between 390 and 430 nm was observed to increase in intensity after UV irradiation and is thus assigned to the neutral C₄Cl molecule.

The 3π and 6σ orbitals are close in energy, resulting in two nearly degenerate states, $2^2\Pi$ and $2^2\Sigma^+$, for the linear form of C₄Cl. The $2^2\Pi$ state is lower in energy by only 7.5 kJ/mol at the CCSD(T) level of theory. The ground state of C₄Cl is predicted to be quasilinear ($2^2A'$) (correlating with the $2^2\Pi$ state), and the barrier to linearity is extremely small (0.7 kJ/mol). The $2^2\Pi$ state has a permanent dipole moment of 4.5 D (CASSCF) which is significantly larger than that of the $2^2\Sigma^+$ state (0.75 D), making it the primary candidate for observation in the neon matrix. The vertical excitation energies below 6 eV and transition moments are listed in Table 1 for transitions originating in the $2^2\Pi$ state of C₄Cl, and the corresponding structure is shown in Figure 1. The appearance of alternating C–C bond lengths suggests that the bonds have polyacetylenic character, as expected for a linear carbon chain.

The band origin in Figure 7 appears at 427.0 nm and is attributed to the $2^2\Pi \leftarrow X^2\Pi$ electronic transition of linear C₄Cl. The assignment is based upon the observation that the band falls within 0.42 eV of the predicted excitation energy and that this transition is expected to be strong. The associated vibrational structure is given in Table 3 and reveals the excitation of three vibrational modes. These modes correspond to the excitation of stretching ($\nu_1 = 1975$ cm⁻¹) and bending ($\nu_4 = 459$ cm⁻¹) modes of the carbon chain and to the C–Cl stretch ($\nu_5 = 317$ cm⁻¹) in the upper electronic state of C₄Cl. The C–Cl stretching frequency of C₄Cl is lower than that measured for C₆Cl (415 cm⁻¹),¹⁵ suggesting that the C–Cl bond is longer in the excited state of the former. This is consistent with ground state calculations which predict a slight shortening of the C–Cl bond with increasing n among the $n = \text{even}$ neutral chains.³ The experimentally determined vibrational frequencies for the excited state of C₄Cl are lower than the calculated values for the ground electronic state (DFT: $\nu_1 = 2175$, $\nu_4 = 555$, and $\nu_5 = 324$ cm⁻¹),³ as observed earlier for other C_{*n*}Cl chains and as expected for electronic promotion to an orbital with a greater number of nodes. Only one mode was observed in the IR spectrum (Figure 8) for the ground electronic state of C₄Cl. This transition is assigned to the C–C stretching mode ($\nu_1 = 2022.1$

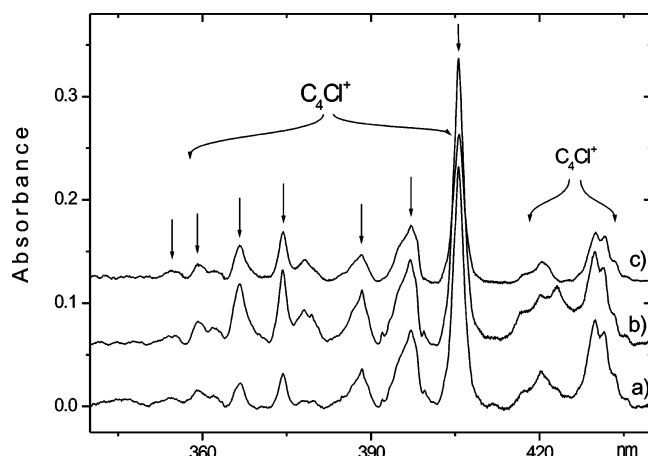


Figure 9. Electronic absorption spectra of the $2^3\Pi \leftarrow X^3\Pi$ electronic transition of C_4Cl^+ recorded after deposition of the cation with neon and CCl_4 to form a 6 K matrix. Traces a and b show the spectra obtained both before and after UV exposure, respectively. Trace c is a difference spectrum of the other two traces scaled to remove the C_4Cl band origin at 427.0 nm.

cm^{-1}), as it compares favorably with the theoretically determined frequency (2175 cm^{-1}) and is slightly larger than the value in the first excited electronic state (1975 cm^{-1}).

The irregular line widths for the transitions in the vibrational progression in Figure 7 are unusual in comparison to the spectra recorded for other members of the C_nCl family.¹⁵ The observed broadening may be a consequence of the interaction of the $2^3\Pi$ ground state with the nearby $2^3\Sigma^+$ state, although the strength of the observed transition certainly suggests that the states involved are predominantly of Π character. The irregular line shapes may also be a result of Fermi resonance contributions.

(e) C_4Cl^+ . As observed for C_3Cl^+ , the spectrum recorded after the deposition of mass-selected C_4Cl^+ ions was dominated by absorptions of neutral species. To observe a clear spectrum of C_4Cl^+ , both N_2O and CCl_4 were added to the neon gas in separate experiments to act as electron scavengers and suppress the neutralization of deposited cations. The spectra of both matrix samples revealed a strong band system between 360 and 410 nm. Figure 9 shows the absorption with CCl_4 present, and the bands assigned to the C_4Cl^+ cation are those that disappear or decrease in intensity after exposure to UV light. A similar spectrum was seen when N_2O was used, confirming that the transitions were not dependent on the added impurity.

In the case of the linear C_4Cl^+ cation, the ground state is $3^3\Sigma^-$ and the nearest state, $3^3\Pi$, is predicted to be approximately 25 kJ/mol (CCSD(T)) and 19 kJ/mol (CCSD) higher in energy. As in the neutral analogue, the Π state has a considerably larger dipole moment and is expected to be stabilized relative to the $3^3\Sigma^-$ ground state in the matrix. Transition moments from the $3^3\Sigma^-$ state of C_4Cl^+ are predicted to be an order of magnitude smaller than those originating in the $3^3\Pi$ state, and thus, only the latter are included in Table 1. The calculated structure of C_4Cl^+ in the $3^3\Pi$ state is shown in Figure 1, and as observed for the neutral counterpart, the carbon backbone of C_4Cl^+ appears to have some polyacetylenic character.

The main band system in Figure 9 is assigned to the $2^3\Pi \leftarrow X^3\Pi$ transition of linear C_4Cl^+ . The origin at 405.7 nm falls within 0.14 eV of the strongest system predicted theoretically. The analogous transition of the isoelectronic C_4S molecule in a neon matrix falls 41 nm to the red of this.¹⁶ A similar red shift (47 nm) was observed upon comparison of the absorption spectra of the longer chains: C_6S and C_6Cl^+ .¹⁵ A second, weaker system, which overlaps with the $2^3\Pi \leftarrow X^3\Pi$ transition of the

neutral C_4Cl chain, is apparent in Figure 9, with the origin band at 431.7 nm. The similar energies observed for the band origins of the neutral and cationic species in Figure 7 are not surprising, given that both observed transitions involve electronic excitations between their 6σ and 3π orbitals. The assignment of the 431.7 nm system is not clear, but it could involve the $3^3\Sigma^+$ or $3^3\Delta$ states calculated to lie nearby (Table 1), the transition gaining intensity from the strong closely located $2^3\Pi \leftarrow X^3\Pi$ system at 405.7 nm.

The vibrational structure observed for the 405.7 nm system of C_4Cl^+ is comparable to that of C_6Cl^+ in a neon matrix,¹⁵ and the positions of the band maxima are listed in Table 3. The bands correspond to the excitation of stretching and bending vibrations involving the carbon chain in the excited electronic state of C_4Cl^+ ($\nu_1 = 2060$, $\nu_2 = 1799$, and $\nu_4 = 534\text{ cm}^{-1}$) and are in good agreement with the calculated ground state values (DFT: $\nu_1 = 2147$, $\nu_2 = 1769$, and $\nu_4 = 583\text{ cm}^{-1}$).³ The C–C stretching frequencies are similar to those reported for the analogous excited state of C_6Cl^+ ($\nu_1 = 2043$, $\nu_2 = 1872\text{ cm}^{-1}$)¹⁵ which suggests that the excited states of these two chains are characterized by similar carbon backbones. The IR absorption spectrum of C_4Cl^+ (Figure 8) reveals two strong vibrational bands at 2034.4 and 1678.0 cm^{-1} which are assigned to the ν_1 and ν_2 modes in the ground electronic state of C_4Cl^+ and are similar to the values reported for the excited state in Table 3.

Conclusion

In this work, electronic absorption spectra of the chlorine-terminated carbon chains C_3Cl , C_3Cl^+ , C_3Cl^- , C_4Cl , and C_4Cl^+ in 6 K neon matrices are reported for the first time. The transitions observed reveal that the neutral C_3Cl radical exists in both bent and cyclic forms in the matrix environment with absorptions in the UV, visible, and NIR regions. The ions of C_3Cl have either bent (C_3Cl^-) or linear (C_3Cl^+) structures and absorb near the visible transition of their neutral analogue. The longer chains, C_4Cl and C_4Cl^+ , appear linear. The spectra presented here provide a more complete set of data to complement existing spectroscopic and theoretical studies of the C_nCl family and serve as a basis for future gas phase spectroscopic measurements which may be used to establish trends in the structures and spectra of heteroatom-terminated carbon chains.

Acknowledgment. This research was supported by the Swiss National Science Foundation (project 200020-100019) as well as the EU project “Molecular Universe” (MRTN-CT-2004-51302). J.v.W. thanks the Natural Science and Engineering Research Council of Canada for postdoctoral support.

References and Notes

- (1) McCarthy, M. C.; Gottlieb, C. A.; Thaddeus, P. *Mol. Phys.* **2003**, *101*, 697.
- (2) Rayon, V. M.; Barrientos, C.; Largo, A. *THEOCHEM* **1998**, *432*, 75.
- (3) Largo, A.; Cimas, A.; Redondo, P.; Barrientos, C. *Int. J. Quantum Chem.* **2001**, *84*, 127.
- (4) Li, G.; Tang, Z. *J. Phys. Chem. A* **2003**, *107*, 5317.
- (5) Redondo, P.; Redondo, J.; Barrientos, C.; Largo, A. *Chem. Phys. Lett.* **1999**, *315*, 224.
- (6) Endo, Y.; Saito, S.; Hirota, E. *J. Mol. Spectrosc.* **1982**, *94*, 199.
- (7) Yamada, C.; Nagai, K.; Hirota, E. *J. Mol. Spectrosc.* **1981**, *85*, 416.
- (8) Burkholder, J. B.; Sinha, A.; Hammer, P. D.; Howard, C. J. *J. Mol. Spectrosc.* **1988**, *127*, 61.
- (9) Jin, P.; Chang, B. C.; Fei, R.; Sears, T. J. *J. Mol. Spectrosc.* **1997**, *182*, 189.
- (10) Venkateswarlu, P. *Phys. Rev.* **1950**, *77*, 79.
- (11) Verma, R. D.; Mulliken, R. S. *J. Mol. Spectrosc.* **1961**, *6*, 419.
- (12) Gordon, R. D.; King, G. W. *Can. J. Phys.* **1961**, *39*, 252.

- (13) Bredohl, H.; Dubois, I.; Melen, F. *J. Mol. Spectrosc.* **1983**, 98, 495.
- (14) Sumiyohsi, Y.; Ueno, T.; Endo, Y. *J. Chem. Phys.* **2003**, 119, 1426.
- (15) van Wijngaarden, J.; Batalov, A.; Shnitko, I.; Fulara, J.; Maier, J. P. *J. Chem. Phys. A* **2004**, 108, 4219.
- (16) Riaplov, E.; Wyss, M.; Lakin, N. M.; Maier, J. P. *J. Phys. Chem. A* **2001**, 105, 4894.
- (17) Maier, J. P. *Chem. Soc. Rev.* **1997**, 26, 21.
- (18) Freivogel, P.; Fulara, J.; Lessen, D.; Forney, D.; Maier, J. P. *Chem. Phys.* **1994**, 189, 335.
- (19) MOLPRO, version 2002.1, a package of ab initio programs designed by H.-J. Werner and P. J. Knowles, with contributions from others; www.molpro.net.
- (20) Kolek, P. Manuscript in preparation.